Hypothesis testing for populations of networks

Li Chen[a], Jie Zhou[b], Lizhen Lin[c*]

[a] *College of Mathematics, Southwest Minzu University, Chengdu, Sichuan, China*

[b] *College of Mathematics, Sichuan University, Chengdu, Sichuan, China*

[c] *Department of Applied and Computational Mathematics and Statistics, University of Notre Dame, South Bend, Indiana, USA*

arXiv:1911.03783v3 [stat.ME] 8 Sep 2021

Abstract: It has become an increasingly common practice in modern science and engineering to collect samples of multiple network data in which a network serves as a basic data object. The increasing prevalence of multiple network data calls for developments of models and theories that can deal with inference problems for populations of networks. In this work, we propose a general procedure for hypothesis testing of networks and in particular, for differentiating distributions of two samples of networks. We consider a very general framework which allows us to perform test on large and sparse networks. Our contribution is two-fold: (1) We propose a test statistics based on the singular value of a generalized Wigner matrix. The asymptotic null distribution of the statistics is shown to follow the Tracy–Widom distribution as the number of nodes tends to infinity. The test also yields asymptotic power guarantee with the power tending to one under the alternative; (2) The test procedure is adapted for change-point detection in dynamic networks which is proven to be consistent in detecting the change-points. In addition to theoretical guarantees, another appealing feature of this adapted procedure is that it provides a principled and simple method for selecting the threshold that is also allowed to vary with time. Extensive simulation studies and real data analyses demonstrate the superior performance of our procedure with competitors.

Keywords: Change-point detection; Dynamic networks; Hypothesis testing; Network data; Tracy–Widom distribution.

1. Introduction

One of the unique features in modern data science is the increasing availability of complex data in non-traditional forms. Among the newer forms of data, network has arguably emerged as one of the most important and powerful data types. A network, an abstract object consisting of a set of nodes and edges, can be broadly used to represent interactions among a set of agents or entities and one can find its applications in virtually any scientific field. The ubiquity of network data in diverse fields ranging from biology (Chen and Yuan, 2006; Cline et al., 2007), physics (Bounova and

*Corresponding author. E-mail: lizhen.lin@nd.edu

de Weck, 2012; Kulig et al., 2015), social science (Hoff et al., 2002; Snijders and Baerveldt, 2003) to engineering (Leonardi and Van De Ville, 2013; Chen et al., 2010) has spurred fast developments in models, theories and algorithms for the field of network analysis, see e.g., Erdős and Rényi (1959); Holland et al. (1983); Karrer and Newman (2011); Ball et al. (2011); Wolfe and Olhede (2013); Rohe et al. (2011); Decelle et al. (2011); Amini and Levina (2018); Bickel and Chen (2009). The existing literature, however, has largely been focusing on inference of one single (often large) network. The recent advancement in technology and computer prowess has led to the increasing prevalence of network data available in multiple networks in which a network serves as the basic data object. For instance, such datasets can be found in neuroscience (Bassett et al., 2008), cancer study (Zhang et al., 2009), microbiome study (Cai et al., 2019), and social interactions (Kossinets and Watts, 2006; Eagle et al., 2009). There is a strong need for development of models and theories that can deal with such data sets, and more broadly, for inference of population of networks.

One has already seen a growing effort in this direction. Ginestet et al. (2017) proposes a geometric framework for hypothesis tests of populations of networks viewing a weighted network as a point on a manifold. Along the same line, Kolaczyk et al. (2020) provides geometric characterization of space of all unlabeled networks which serve as the foundation for inference based on Fréchet mean of networks. In addition, Mukherjee et al. (2017) provides a general framework for clustering network objects. **?** proposes a Gaussian process based framework for regression and classification with network inputs. Durante et al. (2017) proposes a Bayesian nonparametric approach for modeling the populations of networks.

One of commonly encountered problems for inference of populations of networks is hypothesis testing which has significant applications, but remains largely understudied especially for large networks. Among the few existing work in the literature, besides Ginestet et al. (2017) as mentioned above, Tang et al. (2017) carries out hypothesis tests using random dot product graph model via adjacency spectral embedding. Ghoshdastidar et al. (2020) proposes two test statistics based on estimates of the Frobenius norm and spectral norm between link probability matrices of the two samples, the key challenge of which lies in choosing a threshold for the test statistics. Ghoshdastidar and von Luxburg (2018) uses the same statistics as Ghoshdastidar et al. (2020) and proves asymptotic normality for the statistics. Ghoshdastidar and von Luxburg (2018) further proposes a test statistics based on the extreme eigenvalues of a scaled and centralized matrix and proves that the new statistics asymptotically follows the Tracy–Widom law (Tracy and Widom, 1996). Most of the literature, however, focuses on the case where the number of nodes for each network is fixed, which greatly limits the scope of inference.

The initial focus of our work is on hypothesis testing for two samples of networks including

large and sparse networks. We propose a very intuitive testing statistics which yields theoretical guarantees. More specifically, we prove that its asymptotic null distribution follows the Tracy–Widom distribution and the asymptotic power tends to 1 under the alternative. One of the appealing features of our approach is that our test adopts a very general framework in which the number of the nodes are allowed to grow to infinity, while most of the existing methods assume that the number of nodes is fixed, which is not always a practical assumption since many modern networks are often large and sparse. We then adapt our test statistics for a change-point detection procedure in dynamic networks and prove its consistency in detecting change-points. We provide a principled method for selecting the threshold level in the change-point detection procedure based on the asymptotic distribution of the testing statistics and the threshold is allowed to vary with time. This is appealing comparing to many existing change-point detection approaches which require either a cross-validation for selecting the threshold or a careful tuning of the parameters. Extensive simulation studies and two real data analyses demonstrate the superior performance of our procedure in comparing with others in both tasks.

The paper is organized as follows. In Section 2, we propose a testing statistics and throughly study its asymptotic properties. Section 3 is devoted to a change-point detection procedure for dynamic networks by adapting the testing statistics derived in Section 2. Simulation studies are carried out in Section 4 and real data examples are presented in Section 5. Technical proofs can be found in the appendix.

2. Two-sample hypothesis testing for networks

2.1. *Notation*

We first introduce some notations that will be used throughout the paper. For a set $\mathcal{N}$, $|\mathcal{N}|$ denotes its cardinality. TW_1 denotes the Tracy–Widom distribution with index 1. $\chi^2(n)$ denotes the Chi-squared distribution with n degrees of freedom. For a square matrix $B \in \mathbb{R}^{n\times n}$, B_{ij} denotes its (i,j) entry, $B_{i\cdot}$ is the ith row of B, and $B_{\cdot i}$ is the ith column of B. For a symmetric matrix $B \in \mathbb{R}^{n\times n}$, $\lambda_j(B)$ denotes its jth largest eigenvalue, ordered as $\lambda_1(B) \geq \lambda_2(B) \geq \cdots \geq \lambda_n(B)$, $\sigma_1(B)$ is the largest singular value. Write $X_n \rightsquigarrow X$ if a sequence of random variables $\{X_n\}_{n=1}^{\infty}$ converges in distribution to random variable X. $\lfloor x \rfloor$ denotes the largest integer but no greater than $x \in \mathbb{R}$. $I(\cdot)$ denotes indicator function. For two sequences of real numbers $\{x_n\}$ and $\{y_n\}$, we have the following notations:

$y_n = O_n(x_n)$: there exists a positive constant M such that $\lim_{n\to\infty} |\frac{y_n}{x_n}| \leq M$.
$y_n = o_n(x_n)$: $\lim_{n\to\infty} \frac{y_n}{x_n} = 0$.

$y_n = o_p(x_n)$: $\lim_{n\to\infty} P\big(\big|\frac{y_n}{x_n}\big| \geq \varepsilon\big) = 0$ for any positive ε.

2.2. *Problem setup and some existing tests*

We consider two samples of networks with n nodes and sample sizes m_1 and m_2 respectively. More specifically, we assume one observes symmetric binary adjacency matrices $A_1^{(1)}, \ldots, A_1^{(m_1)}$ that are generated from symmetric link probability matrix P_1 with $A_{1,ij}^{(k)} \sim \text{Bernoulli}(P_{1,ij})$, $k = 1, 2, \ldots, m_1$, $i, j = 1, 2, \ldots, n$, and another sample of adjacency matrices $A_2^{(1)}, \ldots, A_2^{(m_2)}$ generated from the same model with link probability matrix P_2. Our goal is to test whether the two samples of networks have same graph structure or not, which is equivalent to testing:

$$H_0 : P_1 = P_2 \text{ against } H_1 : P_1 \neq P_2. \tag{1}$$

For the case of $m_1 = m_2 = 1$ and a fixed n, Tang et al. (2017) focuses on random dot product graphs by applying the adjacency spectral embedding, whereas Ghoshdastidar and von Luxburg (2018) focuses on the inhomogeneous Erdős–Rényi graphs and proposes a test based on eigenvalues.

For the case of large m_1, m_2 and again a fixed number of nodes n, Ginestet et al. (2017) proposes a χ^2-type test based on a geometric characterization of the space of graph Laplacians and a notion of Fréchet means (Fréchet, 1948; Bhattacharya and Lin, 2017). As a simplification of the statistics in Ginestet et al. (2017), Ghoshdastidar and von Luxburg (2018) sets $m_1 = m_2 = m$ and obtains the test statistics as follows:

$$T_{\chi^2} = \sum_{i<j} \frac{(\bar{A}_{1,ij} - \bar{A}_{2,ij})^2}{\frac{1}{m(m-1)} \sum_{k=1}^{m} \left(A_{1,ij}^{(k)} - \bar{A}_{1,ij}\right)^2 + \frac{1}{m(m-1)} \sum_{k=1}^{m} \left(A_{2,ij}^{(k)} - \bar{A}_{2,ij}\right)^2}, \tag{2}$$

where $\bar{A}_{u,ij} = \frac{1}{m} \sum_{k=1}^{m} A_{u,ij}^{(k)}$ with $u = 1, 2$. Then $T_{\chi^2} \to \chi^2\big(\frac{n(n-1)}{2}\big)$ as $m \to \infty$. We call this method χ^2-type test.

The case of large n and fixed m_1 and m_2 is one of the likely scenarios in practice and is thus perhaps more interesting. Ghoshdastidar and von Luxburg (2018) uses the same statistics as Ghoshdastidar et al. (2020) as follows:

$$T_N = \frac{\sum_{i<j} \left(\sum_{k\leq m/2} A_{1,ij}^{(k)} - A_{2,ij}^{(k)}\right) \left(\sum_{k>m/2} A_{1,ij}^{(k)} - A_{2,ij}^{(k)}\right)}{\sqrt{\sum_{i<j} \left(\sum_{k\leq m/2} A_{1,ij}^{(k)} + A_{2,ij}^{(k)}\right) \left(\sum_{k>m/2} A_{1,ij}^{(k)} + A_{2,ij}^{(k)}\right)}}. \tag{3}$$

Ghoshdastidar and von Luxburg (2018) proves the asymptotic normality of T_N as $n \to \infty$. We refer this method to N-type test.

2.3. *Proposed test statistics*

In proposing our test statistics, we consider a very general setting in which the number of nodes can grow to infinity instead of being fixed like in most of the existing literature, and the sample sizes m_1 and m_2 grow in an appropriate rate. We first introduce the centralized and re-scaled matrix Z with entries given as follows:

$$Z_{ij} = \frac{\bar{A}_{1,ij} - \bar{A}_{2,ij}}{\sqrt{(n-1)\left[\frac{1}{m_1}P_{1,ij}\big(1-P_{1,ij}\big) + \frac{1}{m_2}P_{2,ij}\big(1-P_{2,ij}\big)\right]}}, \tag{4}$$

where $\bar{A}_{u,ij} = \frac{1}{m_u}\sum_{k=1}^{m_u} A_{u,ij}^{(k)}$ with $u = 1, 2$ and $i, j = 1, \ldots, n$.

The matrix Z involves unknown link probability matrices P_1 and P_2 thus can not be directly used as a test statistics. As an alternative, one can choose some appropriate plugin estimates for P_1 and P_2, and some of these estimates attain good properties for the resulting tests as we will see in the following discussions.

Denote $\hat{P}_1$ and $\hat{P}_2$ as some plugin estimators of P_1 and P_2 respectively, then the empirical standardized matrix $\hat{Z}$ of Z can be written with entries as

$$\hat{Z}_{ij} = \frac{\bar{A}_{1,ij} - \bar{A}_{2,ij}}{\sqrt{(n-1)\left[\frac{1}{m_1}\hat{P}_{1,ij}\big(1-\hat{P}_{1,ij}\big) + \frac{1}{m_2}\hat{P}_{2,ij}\big(1-\hat{P}_{2,ij}\big)\right]}},\ i, j = 1, 2, \ldots, n. \tag{5}$$

We propose to use the largest singular value of $\hat{Z}$, after suitable shifting and scaling, as our test statistics:

$$T_{TW_1} = n^{2/3}\big[\sigma_1(\hat{Z}) - 2\big]. \tag{6}$$

Given a significance level $\alpha \in (0, 1)$, the rejection region Q for H_0 in test (1) is

$$Q = \{T_{TW_1} | T_{TW_1} \geq \tau_{\alpha/2}\}, \tag{7}$$

where $\tau_{\alpha/2}$ is the corresponding $\alpha/2$ upper quantile of TW_1. We then have the following results.

Theorem 2.1 (General asymptotic null distribution)**:** *Let $A_1^{(1)}, \ldots, A_1^{(m_1)}$ be a sample of networks generated from a link probability matrix P_1 with n nodes, and $A_2^{(1)}, \ldots, A_2^{(m_2)}$ be another sample generated from a link probability matrix P_2 with the same number of nodes. Let $\hat{Z}$ be given as in* (5)*. Given some estimated matrices $\hat{P}_u$ of $P_u, u = 1, 2$, if $\sup_{i,j} |\hat{P}_{u,ij} - P_{u,ij}| = o_p(n^{-2/3})$, then the following holds under the null hypothesis in* (1)*:*

$$n^{2/3}[\lambda_1(\hat{Z}) - 2] \rightsquigarrow TW_1,\ n^{2/3}[-\lambda_n(\hat{Z}) - 2] \rightsquigarrow TW_1. \tag{8}$$

Remark 2.2: *Theorem 2.1 is very general in the sense that it puts no structural conditions on the networks, nor does it impose any assumption on the type of estimates for P_1 and P_2 so long as they are estimated within $o_p(n^{-2/3})$ error.*

The following corollaries show asymptotic type I error control and asymptotic power for the rejection rule (7).

Corollary 2.3 (Asymptotic type I error control)**:** *Supposing assumptions in Theorem 2.1 hold, the rejection region in* (7) *has size α.*

Corollary 2.4 (Asymptotic power guarantee)**:** *Define a matrix $\tilde{Z} \in \mathbb{R}^{n\times n}$ with zero diagonal and for any $i \neq j$,*

$$\tilde{Z}_{ij} = \frac{P_{1,ij} - P_{2,ij}}{\sqrt{(n-1)\Big[\frac{1}{m_1}P_{1,ij}\big(1-P_{1,ij}\big) + \frac{1}{m_2}P_{2,ij}\big(1-P_{2,ij}\big)\Big]}}. \tag{9}$$

Under the assumptions of Theorem 2.1, if $P_{1,ij}$ and $P_{2,ij}$ are such that $n^{-2/3}[\sigma_1(\tilde{Z}) - 4]^{-1} \leq o_n(1)$, then

$$P(T_{TW_1} \geq \tau_{\alpha/2}) = 1 - o_n(1).$$

Remark 2.5: *As mentioned in the introduction, in Ghoshdastidar and von Luxburg (2018), a test statistics for comparing two large graphs is proposed, and our test statistics appears to be similar in natural to theirs. However, there are some key distinctions between our method and theirs. First, our testing statistics considers two-sample test on two populations of networks which requires exploration of the proper interplay between the asymptotics in both the sample sizes of networks and nodes number. Second, Ghoshdastidar and von Luxburg (2018) proves the asymptotic Tracy–Widom law under the true link probability matrices, while in our paper, we consider various estimates of link probability matrices (again based on multiple networks) and prove the Tracy–Widom law theoretically. We also discuss the performance of the resulting testing statistics under various estimators. Third, our testing statistics is modified for a novel and efficient change-point detection procedure and the consistency of the change-point detection is also proved.*

2.4. *Different estimators of link probability matrix*

The testing statistics proposed in the previous section requires a plugin estimator for the link probability matrix based on a sample of networks. In this subsection, we investigate the properties of the tests corresponding to various different estimators for link probability matrix.

We first consider a different but natural and simple estimator of P_u by using the average of all the adjacency matrices in the same group. We denote this method as AVG and the link probability matrix estimator as $\hat{P}_{\mathrm{AVG},u}$, which is actually $\bar{A}_u$.

It's not difficult to see that

$$\sup_{i,j} |\hat{P}_{\mathrm{AVG},u,ij} - P_{u,ij}| = o_p\big(m_u^{-1/2} \log(n)\big)$$

by applying Bernstein's inequality. To guarantee the asymptotic TW_1 in (8), it requires that $m_u = O_n(n^{4/3})$. More specifically, the sample size m_u needs to increase faster than nodes number n, so m_u will exceed n eventually as n tends to infinity. Therefore, the AVG estimator will perform well if the sample size is large enough. However, this is hard to hold in reality especially when the size of the network is large. Usually, for most practical applications, it would be more suitable to require m_u to increase slower than n.

We also consider an average estimator of P_u based on the stochastic block model (SBM), which is similar in spirit to the estimator in Ghoshdastidar and von Luxburg (2018) but with a different algorithm for estimating the communities. Our main idea can be summarized as follows: First, assume the graphs are SBMs, or approximate them with SBMs by a weaker version of Szemerédi's regularity lemma (see Lovász (2012)). Second, use one of the community detection algorithms such as the goodness-of-fit test proposed in Lei (2016) to estimate the number of the communities $\hat{K}_u$. Then perform clustering using for example the spectral clustering algorithm (see, e.g., von Luxburg (2007)) to obtain estimates of the membership vector $g_u \in \{1, \ldots, \hat{K}_u\}^n$ as well as the community set $\mathcal{B}_{u,k} = \{i : 1 \le i \le n, g_{u,i} = k\}$, where $k = 1, 2, \ldots, \hat{K}_u$ and $g_{u,i}$ is the ith element of g_u. Subsequently, P_u is approximated by a block matrix $\hat{P}_{\mathrm{SBM},u}$ such that $\hat{P}_{\mathrm{SBM},u,ij}$ is the mean of the submatrix of $\bar{A}_u$ restricted to $\mathcal{B}_{u,g_{u,i}} \times \mathcal{B}_{u,g_{u,j}}$.

Under further assumption that each community has size at least proportional to n/K_u, where K_u is the true community number, it can be seen that the error of $\hat{P}_{\mathrm{SBM},u,ij}$ is $o_p(K_u m_u^{-1/2} n^{-1} \log n)$ (Lei, 2016). This implies that only when $K_u = O_n(n^{\gamma_u}), \gamma_u < 1/3 + \alpha_u/2$, and $m_u = O_n(n^{\alpha_u}), \alpha_u \ge 0$, the error condition in Theorem 2.1 holds. For large networks in practice, the number of communities can be very large therefore such a condition might be hard to satisfy. Moreover, due to the potential double estimation in the process (in estimating the number of communities as well as the community membership), it may bring large error to the final test statistics, especially when the SBM assumption is not valid.

We now discuss another explicit method for the link probability matrix estimates that can be used as the plugging estimates in the test statistics called the modified neighborhood smoothing (MNBS) estimator. Let $\{\xi_i\}_{i=1}^n$ be a random sequence such that $\xi_i, i = 1, \ldots, n$, are *i.i.d.* uniform random

variables on $[0,1]$. Conditional on this global sequence $\{\xi_i\}_{i=1}^n$, we assume all the adjacency matrices $A^{(1)}, A^{(2)}, \ldots, A^{(m)}$ in the same population share the same link probability matrix $P \in \mathbb{R}^{n\times n}$, which is modeled by a graphon function $f : [0,1]^2 \to [0,1]$ such that

$$P_{ij} = f(\xi_i, \xi_j).$$

Therefore, we have

$$A_{ij}^{(k)} \mid \{\xi_i\}_{i=1}^n \sim \text{Bernoulli}(f(\xi_i, \xi_j)),$$

independently for all $i \le j$ and $k = 1, \ldots, m$.

We then apply MNBS method proposed in Zhao et al. (2019) to estimate P. The essential idea of the MNBS procedure consists of the following steps: First, for the group of adjacency matrices $A^{(1)}, A^{(2)}, \ldots, A^{(m)}$ generated from P, let $\bar{A} = \sum_{k=1}^m A^{(k)}/m$, define the distance measure between nodes i and i' as $d^2(i,i') = \max_{k\neq i,i'} |\langle \bar{A}_{i\cdot} - \bar{A}_{i'\cdot}, \bar{A}_{k\cdot}\rangle|$ and the neighborhood of node i as $\mathcal{N}_i = \{i' \neq i : d^2(i,i') \le q_i(q)\}$, where $q_i(q)$ denotes the qth quantile of the distance set $\{d^2(i,i') : i' \neq i\}$. Then the parameter q is set to be $C\log n/(n^{1/2}\omega)$, where C is some positive constant and $\omega = \min\{n^{1/2}, (m\log n)^{1/2}\}$. Finally, given the neighborhood $\mathcal{N}_i$ for each node i, the link probability P_{ij} between nodes i and j is estimated by $\tilde{P}_{ij} = \sum_{i'\in\mathcal{N}_i} \bar{A}_{i'j}/|\mathcal{N}_i|$. In comparing with the neighborhood smoothing method proposed in Zhang et al. (2017), the key idea is to employ the average network information $\bar{A}$ and simultaneously shrink the neighborhood size (from $C(\log n/n)^{1/2}$ to $C\log n/(n^{1/2}\omega)$) to obtain an estimate with an improved rate.

Based on MNBS, for the symmetric networks considered in this paper, we use symmetrized estimators of the link probability matrices $P_u, u = 1, 2$, of the two groups of graphs as

$$\hat{P}_u = \frac{\tilde{P}_u + (\tilde{P}_u)^T}{2}, \text{ with } \tilde{P}_{u,ij} = \frac{\sum_{i'\in\mathcal{N}_{u,i}} \bar{A}_{u,i'j}}{|\mathcal{N}_{u,i}|}, \tag{10}$$

where $\bar{A}_{u,i'j}$ is the (i',j) element of $\bar{A}_u = \sum_{k=1}^{m_u} A_u^{(k)}/m_u$ and $\mathcal{N}_{u,i}$ is the neighborhood of node i in group u.

From Lemma 9.3 in Zhao et al. (2019), we have

$$|\mathcal{N}_{u,i}| \ge B_u \frac{n^{1/2}\log n}{\omega_u}, \tag{11}$$

where B_u is a global positive constant and $\omega_u = \min\{n^{1/2}, (m_u \log n)^{1/2}\}$ for $u = 1, 2$.

For the MNBS, we do not provide an explicit rate on bounding the sup norm $\sup_{i,j} |\hat{P}_{u,ij} - P_{u,ij}|$ due to the difficulty in deriving the point-wise rate. From the definition of $d^2(i,i')$, it can be seen

that the distance measure between nodes i and i' in the MNBS algorithm is based on the row pattern similarity instead of point-wise way. To derive an entry-wise error of P_{ij}, one can use Bernstein's inequality, but the neighbor of a node is selected by the qth quantile of the distance set, which would decrease the variance of sample in the neighbor, but this decreased variance is unknown. The extensive simulation carried out in Section 4 and Section 5 show that MNBS-based tests often yield the best performance in comparing with tests based on other estimators.

Remark 2.6: *As one can see in our setup in Section 2.2, it is assumed that the edges of each network $A^{(k)}$, $k = 1, \ldots, m$, in the same populations are generated* independently *from the same deterministic link probability matrix P. To fit this setup under a genuine 'graphon model', one has to assume that for each node i, the latent variable ξ_i is the same over all the samples in the same population and will not change for each sample. That is, a global latent sequence $\{\xi_i\}_{i=1}^n$ is shared across all the networks. Note that this setup does not fall under a genuine graphon model in which one first samples uniform random sequence $\{\xi_i^{(k)}\}_{i=1}^n$ for each network over k, then $A_{ij}^{(k)} \mid \{\xi_i^{(k)}\}_{i=1}^n \sim Bernoulli(f(\xi_i^{(k)}, \xi_j^{(k)}))$. Therefore, the entries of the adjacent matrix or network are not independent after marginalizing the latent variables.*

3. Change-point detection in dynamic networks

We refer the two sample test based on asymptotic TW_1 proposed in the previous section as TW_1-type test. In this section, we adapt the TW_1-type test to a procedure for change-point detection in dynamic networks, which is another important learning task in statistics and has received a great deal of recent attentions. Specifically, we examine a sequence of networks whose distributions may exhibit changes at some time epochs. Then, the problem is to determine the unknown change-points based on the observed sequence of network adjacency matrices.

Assume the observed dynamic networks $\{A_t\}_{t=1}^m$ are generated by a sequence of probability matrices $\{P_t\}_{t=1}^m$ with $A_{t,ij} \sim \text{Bernoulli}(P_{t,ij})$ for time $t = 1, \ldots, m$. Let $\mathcal{J} = \{\eta_j\}_{j=1}^J \subset \{1, \ldots, m\}$ be a collection of change-points and $\eta_0 = 0$, $\eta_{J+1} = m$, ordered as $\eta_0 < \eta_1 < \cdots < \eta_J < \eta_{J+1}$, such that

$$P_t = P^{(j)}, t = \eta_{j-1} + 1, \ldots, \eta_j, j = 1, \ldots, J+1.$$

In other words, the change-points $\{\eta_j\}_{j=1}^J$ divide the networks into $J+1$ groups, the networks contained in the same group follow the same link probability matrix and $P^{(j)}$ is the link probability matrix of the jth segment satisfying $P^{(j)} \neq P^{(j+1)}$. Denote $\mathcal{J} = \varnothing$ if $J = 0$.

Now we apply our TW_1-type test to a screening and thresholding algorithm that is commonly used in change-point detection, see Niu and Zhang (2012); Zou et al. (2014); Zhao et al. (2019). The detection procedure is referred as TW_1-type detection and described as follows.

Define $L = \min_{1\le j\le J+1}(\eta_j - \eta_{j-1})$, which is the minimum segment length. Set a screening window size $h \ll m$ and $h < L/2$. Denote $\bar{A}_1(t,h) = \frac{1}{h}\sum_{i=t-h+1}^{t} A_i$ and $\bar{A}_2(t,h) = \frac{1}{h}\sum_{i=t+1}^{t+h} A_i$ for each $t = h, \ldots, m-h$. $\hat{P}_1(t,h)$ and $\hat{P}_2(t,h)$ are for example MNBS estimators using $\{A_i\}_{i=t-h+1}^{t}$ and $\{A_i\}_{i=t+1}^{t+h}$ respectively. In addition, we denote a matrix $\hat{Z}(t,h)$ with entries as follows essentially the same as in (5):

$$\hat{Z}_{ij}(t,h) = \frac{\bar{A}_{1,ij}(t,h) - \bar{A}_{2,ij}(t,h)}{\sqrt{(n-1)\left\{\frac{1}{h}\hat{P}_{1,ij}(t,h)\Big[1-\hat{P}_{1,ij}(t,h)\Big] + \frac{1}{h}\hat{P}_{2,ij}(t,h)\Big[1-\hat{P}_{2,ij}(t,h)\Big]\right\}}},$$
$$i,j = 1,2,\ldots,n.$$

In the screening step, we calculate the scan statistics $T_{TW_1}(t,h)$ depending only on observations in a small neighborhood $[t-h+1, t+h]$ as follows:

$$T_{TW_1}(t,h) = n^{2/3}\big\{\sigma_1\big[\hat{Z}(t,h)\big] - 2\big\}.$$

Define the h-local maximizers of $T_{TW_1}(t,h)$ as $\{t : T_{TW_1}(t,h) \ge T_{TW_1}(t',h) \text{ for all } t' \in (t-h, t+h)\}$. Let $\mathcal{LM}$ denote the set of all h-local maximizers of $T_{TW_1}(t,h)$.

In the thresholding step, we estimate the change-points by a thresholding rule to $\mathcal{LM}$ with time t such that

$$\hat{\mathcal{J}} = \{t : t \in \mathcal{LM} \text{ and } T_{TW_1}(t,h) > \triangle_{T_{TW_1}}\}, \tag{12}$$

where $\triangle_{T_{TW_1}} = \max\{\tau_\alpha, n^{2/3}[\delta(t,h) - 4] - \tau_\alpha\}, \alpha = 1/2 - (1-1/n)^{1/(2h)}/2, \delta(t,h) = \sigma_1(V_1(t,h))$ is the largest singular value of matrix $V_1(t,h)$ with zero diagonal and for any $i \ne j$,

$$V_{1,ij}(t,h) = \frac{\hat{P}_{1,ij}(t,h) - \hat{P}_{2,ij}(t,h)}{\sqrt{(n-1)\Big\{\frac{1}{h}\hat{P}_{1,ij}(t,h)\Big[1-\hat{P}_{1,ij}(t,h)\Big] + \frac{1}{h}\hat{P}_{2,ij}(t,h)\Big[1-\hat{P}_{2,ij}(t,h)\Big]\Big\}}},$$
$$i,j = 1,2,\ldots,n.$$

We have the following consistency result.

Theorem 3.1 (Consistency of TW_1-type change-point detection)**:** *Under the alternative hypothesis, assume* $n^{2/3}[\sigma(t,h)-4] \ge 2\tau_\alpha, \alpha = 1/2-(1-1/n)^{1/(2h)}/2, h < L/2$*, then the* TW_1*-type change-point*

detection procedure satisfies

$$\lim_{n\to\infty} P\big(\mathcal{J} = \hat{\mathcal{J}}\big) = 1.$$

One of the interesting findings from Theorem 3.1 is that for a fixed window size h, the threshold in (12) is dynamic with time t instead of being a constant as in Zhao et al. (2019). By adapting the TW_1-type test for change-point detection, we can adjust the threshold with t and still enjoy consistency of the change-point detection. From the proof of Theorem 3.1, it is reflected that for a time t that does not correspond to a change-point, $T_{TW_1}(t,h) \leq \triangle_{T_{TW_1}}$ with probability 1, so it can control the type I error. However, for a change-point t, $T_{TW_1}(t,h) > \triangle_{T_{TW_1}}$ with probability 1, and hence the threshold can lead to a good performance.

The only tuning parameter of TW_1-type change-point detection procedure is the local window size h, which is chosen according to applications with available information or artificially like set $h = \sqrt{m}$ as recommended in Zhao et al. (2019).

4. Simulation study

In this section, we illustrate the performance of TW_1-type test and its application to change-point detection using several synthetic data examples.

We first define four graphons and an SBM, which are used for two-sample test and change-point detection in the simulation studies. The graphons are partly borrowed from Zhang et al. (2017) and the SBM is from Zhao et al. (2019) with 2 communities. We denote the block matrix or the probability matrix of connections between blocks as Λ. More specifically, the graphons and SBM are defined as:

Graphon 1:

$$f(u,v) = \begin{cases} k/(K+1), & u,v \in ((k-1)/K, k/K), \\ 0.3/(K+1), & \text{otherwise}, \end{cases}$$

where $K = \lfloor \log n \rfloor, k = 1, 2, \ldots, K$.

Graphon 2:

$$f(u,v) = (u^2+v^2)/3\cos[1/(u^2+v^2)] + 0.15.$$

Graphon 3:

$$f(u,v) = \sin[5\pi(u+v-1)+1]/2 + 0.5.$$

Graphon 4:

$$f(u,v) = (u^2+v^2)/10\cos[1/(u^2+v^2)] + 0.05.$$

SBM 1:

$$\Lambda = \begin{bmatrix} 0.6+\theta_0 & 0.3 \\ 0.3 & 0.6 \end{bmatrix},$$

where θ_0 is a constant related to sample size m. The membership of the ith node is $M(i) = I(1 \leq i \leq \lfloor 2n/\log n \rfloor) + 2I(\lfloor 2n/\log n \rfloor + 1 \leq i \leq n)$.

To operationalize simulations related to MNBS, the quantile parameter $q = B_0(\log n)^{1/2}/(n^{1/2}h^{1/2})$ and the threshold $\triangle_D = D_0(\log n)^{1/2+\delta_0}/(n^{1/2}h^{1/2})$ with tuning parameters D_0 and δ_0 for change-point detection in Zhao et al. (2019) need to be specified. In the following simulations in this section and the real data analyses in Section 5, we set the related parameters $h = \sqrt{m}, B_0 = 3, \delta_0 = 0.1, D_0 = 0.25$ as recommended in Zhao et al. (2019) unless otherwise indicated.

4.1. *Two-sample test with simulated data*

To examine the performance of the two-sample test (1), we present our results by TW_1-type tests based on MNBS (TW_1-MNBS), AVG (TW_1-AVG), and SBM (TW_1-SBM) discussed in subsection 2.4, χ^2-type test with statistics (2), and N-type test with statistics (3). We measure the performance in terms of the Attained Significance Level (ASL) which is the probability of observing a statistics far away from the true value under the null hypothesis, and the Attained Power (AP), the probability of correctly rejecting the null hypothesis when the alternative hypothesis is true.

We conduct two experiments using Graphon 1 and Graphon 2 respectively. In the first experiment, we generate two groups of networks $\{A_1^{(k)}\}_{k=1}^{m_1}$ and $\{A_2^{(k)}\}_{k=1}^{m_2}$. We vary the number of nodes n growing from 100 to 1000 in a step of 100 with sample sizes $m_1 = m_2 = 30, 200$, and set significance level at $\alpha = 0.05$. $\{A_1^{(k)}\}_{k=1}^{m_1}$ are generated from Graphon 1. Under the null hypothesis, $\{A_2^{(k)}\}_{k=1}^{m_2}$ are also generated from the Graphon 1 and hence $P_1 = P_2$. Under the alternative hypothesis, randomly choose $\lfloor \log n \rfloor$-element subset $S \subset \{1, 2, \ldots, n\}$, generate $\{A_2^{(k)}\}_{k=1}^{m_2}$ from P_2 by setting $P_{2,ij} = P_{1,ij} + \theta_1$ with $\theta_1 = 0.05$ for $m_1 = m_2 = 30$ ($\theta_1 = 0.02$ for $m_1 = m_2 = 200$) if $i, j \in S$, and $\theta_1 = 0$ otherwise. Using TW_1-MNBS, TW_1-AVG, TW_1-SBM tests, χ^2-type test and N-type test, we run 1000 Monte Carlo simulations for the experiment to estimate the ASLs and APs of test (1).

The second experiment is conducted similarly but using Graphon 2. The only difference is that for a better visualization of comparisons, under the alternative hypothesis, we set $P_{2,ij} = P_{1,ij} + \theta_2$ with $\theta_2 = 0.2$ for $m_1 = m_2 = 30$ ($\theta_2 = 0.17$ for $m_1 = m_2 = 200$) if $i, j \in S$ and $\theta_2 = 0$ otherwise. The rates of rejecting the null hypothesis for these two experiments are summarized in Figures 1 and 2 respectively.

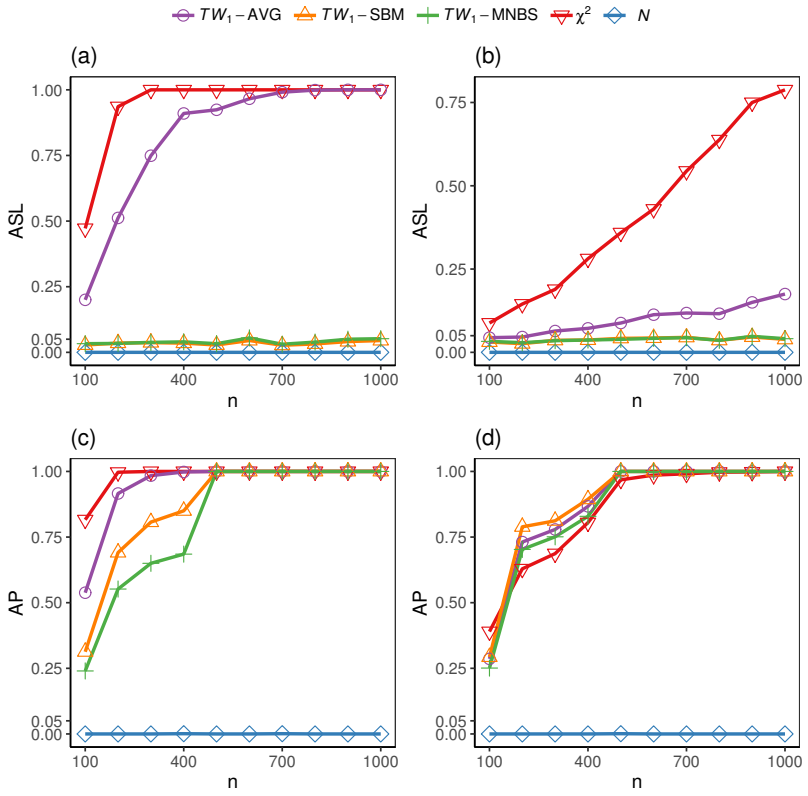


Figure 1. ASLs and APs of tests using Graphon 1 for different values of nodes number n, sample sizes m_1 and m_2. $m_1 = m_2 = 30$ for (a) and (c) and $m_1 = m_2 = 200$ for (b) and (d).

The results of the first experiment using Graphon 1, an SBM set up, are plotted in Figure 1. It reveals undesirable behaviors of χ^2-type test and TW_1-AVG test since with increasing number of nodes n, the ASLs of both tests grow quickly close to 1, which is too large to be used in practice. We can also see that the N-type test is not efficient as both ASLs and APs of the test are 0 for both cases of $m_1 = m_2 = 30, 200$. Its poor performance in APs is partly due to the small difference between $\{A_1^{(k)}\}_{k=1}^{m_1}$ and $\{A_2^{(k)}\}_{k=2}^{m_2}$ we set. However, the performance of TW_1-SBM test and TW_1-MNBS test are much better, ASLs of both tests are stable and close to the significance level of $\alpha = 0.05$, while APs improve to 1 as n grows. It is also found that when n is not that large, TW_1-SBM test is slightly more powerful in terms of AP than TW_1-MNBS test. This is not surprising because the networks generated from Graphon 1 are endowed with an SBM structure.

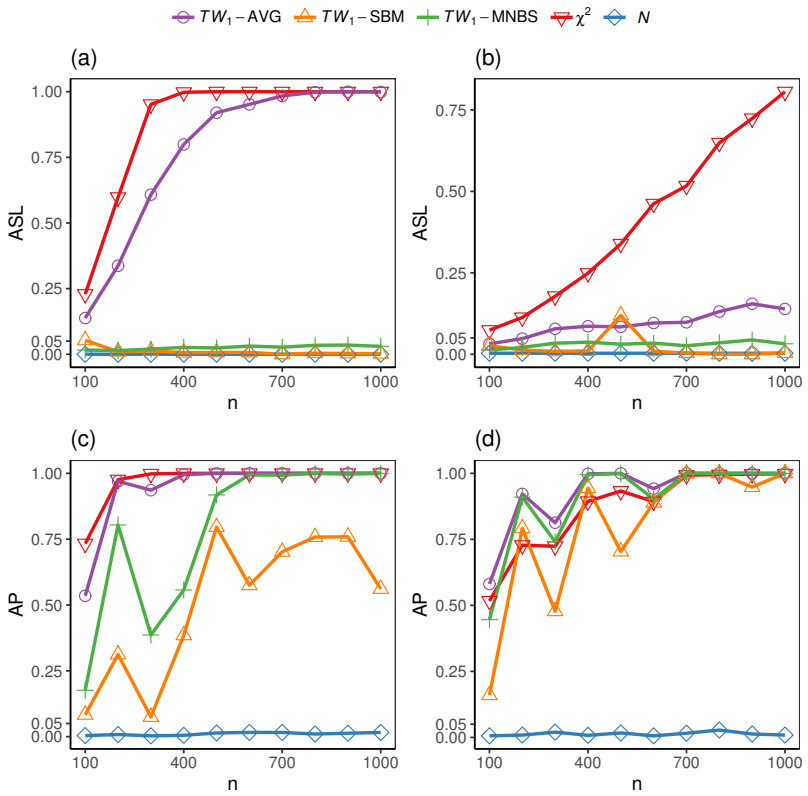


Figure 2. ASLs and APs of tests using Graphon 2 for different values of nodes number n, sample sizes m_1 and m_2. $m_1 = m_2 = 30$ for (a) and (c) and $m_1 = m_2 = 200$ for (b) and (d).

The results of the second experiment using Graphon 2, which is not an SBM, are given in Figure 2. It indicates that the behaviors of TW_1-AVG test, χ^2-type test and N-type test are similar to those in the first experiment using Graphon 1 and the performance is poor. On the other hand, TW_1-MNBS test has a superior performance than TW_1-SBM in both ASL and AP. Specifically, ASLs of TW_1-SBM test are away from 0.05, whereas TW_1-MNBS test still performs well on both ASL and AP. Moreover, this also indicates that TW_1-SBM test is sensitive to the network structure especially deviation from an SBM. Hence, TW_1-MNBS test is more robust to the network structure whereas TW_1-SBM test is preferable for SBM networks.

4.2. *Change-point detection in dynamic networks*

To assess the performance of TW_1-type change-point detection in dynamic networks, we compare its performance based on MNBS, AVG, and SBM estimators (referred as CP-TWMNBS, CP-TWAVG, CP-TWSBM respectively) to the graph-based nonparametric testing procedure in Chen and Zhang (2015) referred as CP-GRA detection, and the MNBS-based change-point detect procedure in Zhao

et al. (2019) referred as CP-DMNBS detection.

Specifically, using all the above five methods, we conduct change-point detection experiments under three different scenarios with zero, one, and three change-points respectively. For all the experiments, we vary the nodes number and the sample size at $n = 100, 200, 300, m = 100, 200$, and set the significance $\alpha = 0.05$. For each combination of the sample size, nodes number, and the network model, we run 100 Monte Carlo trials. Simultaneously, we also explore the effect of network sparsity on the performance of change-point detection. For this, we consider the above setting, but scale the link probability P as ρP by a factor $\rho = 1, 0.25$, where $\rho = 1$ is exactly the same as the above setting while $\rho = 0.25$ corresponds to sparser graphs.

4.2.1. No change-point detection

To study the performance with respect to false positives, we simulate two kinds of dynamic networks $\{A_t\}_{t=1}^m$ with no change-point from Graphon 3 and SMB 1 with $\theta_0 = 0$ respectively. Tables 1 and 2 report the average number of estimated change-points by using the five methods .

As one can see, the performance of CP-TWSBM, CP-TWMNBS, and CP-GRA detections perform reasonably well and improves as n increases. CP-TWAVG detect method performs well in the case of Graphon 3 while experiences heavy inflated levels in the case of SBM 1. As for CP-DMNBS detection, the empirical type I error is completely controlled at the target level 0.05 for SBM 1, but there are some false positives in the case of Graphon 3.

Table 1. Average estimated change-points number $\hat{J}$ under no change-point scenarios through Graphon 3.

m	n	ρ	CP-TWAVG	CP-TWSBM	CP-TWMNBS	CP-GRA	CP-DMNBS
100	100	1	0.00	0.00	0.00	0.04	3.75
		0.25	0.00	0.00	0.00	0.03	2.04
100	200	1	0.00	0.00	0.00	0.11	0.15
		0.25	0.00	0.00	0.00	0.07	0.3
100	300	1	0.00	0.00	0.00	0.04	0.02
		0.25	0.00	0.00	0.00	0.04	0.02
200	100	1	0.00	0.00	0.00	0.02	2.02
		0.25	0.00	0.00	0.00	0.08	5.16
200	200	1	0.00	0.00	0.00	0.08	0.21
		0.25	0.00	0.00	0.00	0.03	0.35
200	300	1	0.00	0.00	0.00	0.05	0.01
		0.25	0.00	0.00	0.00	0.08	0.01

4.2.2. Single change-point detection

We now assess the accuracy of our proposed TW_1-type change-point estimators in different scenarios. The dynamic networks $\{A_t\}_{t=1}^m$ are designed as follows. For $t = 1, 2, \ldots, m/2$, A_t is generated from link probability matrix P_1 by SBM 1 with $\theta_0 = 0$. For $t = m/2 + 1, \ldots, m$, A_t is

Table 2. Average estimated change-points number $\hat{J}$ under no change-point scenarios through SBM 1.

m	n	ρ	CP-TWAVG	CP-TWSBM	CP-TWMNBS	CP-GRA	CP-DMNBS
100	100	1	4.19	0.02	0.02	0.10	0.00
		0.25	0.06	0.02	0.02	0.02	0.00
100	200	1	4.21	0.00	0.00	0.04	0.00
		0.25	0.16	0.00	0.03	0.03	0.00
100	300	1	4.09	0.01	0.01	0.04	0.00
		0.25	0.17	0.02	0.03	0.01	0.00
200	100	1	5.74	0.02	0.02	0.08	0.00
		0.25	0.42	0.02	0.07	0.04	0.00
200	200	1	6.34	0.03	0.03	0.07	0.00
		0.25	1.13	0.02	0.02	0.01	0.00
200	300	1	6.26	0.02	0.02	0.03	0.00
		0.25	2.30	0.01	0.01	0.02	0.00

generated from P_2 by SBM 1 with $\theta_0 = -m^{-1/4}$.

We adopt Boysen distance suggested in Boysen et al. (2009) as a measurement in the change-point estimation. Specifically, calculate the distances between the estimated change-point set $\hat{\mathcal{J}}$ and the true change-point set $\mathcal{J}$ as $\varepsilon(\hat{\mathcal{J}}\|\mathcal{J}) = \max_{b\in\mathcal{J}} \min_{a\in\hat{\mathcal{J}}} |a-b|$ and $\varepsilon(\mathcal{J}\|\hat{\mathcal{J}}) = \max_{b\in\hat{\mathcal{J}}} \min_{a\in\mathcal{J}} |a-b|$.

Utilizing CP-TWMNBS, CP-TWAVG, CP-TWSBM, CP-GRA, and CP-DMNBS detections, we estimate the efficient detect rate (the rate at least one change-point is detected over 100 simulations), the average change-point number over the efficient detections, and the average Boysen distances over the efficient detections. The corresponding results are listed in Tables 3–5.

Results provided in Tables 3–5 show that CP-TWSBM and CP-TWMNBS detections yield reliable estimates of the number of change-points and their locations. When $\rho = 1$, CP-TWAVG over-estimates the number of change-points, but it's interesting that it performs well for sparser case of $\rho = 0.25$. A possible explanation is that the sparser structure overcomes its inflated behavior to some extent. As for CP-GRA and CP-DMNBS detections, the performances of both methods are reasonable in dense scenarios, especially CP-DMNBS. However, they are unable to detect any change-point for the sparser setting $\rho = 0.25$ in this example.

4.2.3. Three change-points detection

To assess the robustness of our method for change-point detection, we further construct a model with three change-points in the networks. We first design three types of link probability matrix changes, which we use to build dynamic networks later. Given a link probability matrix P, define a changed link probability matrix initialized as $P' = P$. For two given sets $\mathcal{M}_1, \mathcal{M}_2 \subset \{1, 2, \ldots, n\}$, for any $i \in \mathcal{M}_1$ and $j \in \mathcal{M}_2$, the different types of link probability matrix changes are defined as follows:

Table 3. Average estimated change-points number $\hat{J}$ under single change-point scenarios through SBM 1.

m	n	ρ	CP-TWAVG	CP-TWSBM	CP-TWMNBS	CP-GRA	CP-DMNBS
100	100	1	3.43	1.01	1.01	1.07	1.00
		0.25	1.02	0.95	0.98	0.00	0.00
100	200	1	3.50	1.01	1.01	1.09	1.00
		0.25	1.04	1.00	1.01	0.00	0.00
100	300	1	3.49	1.01	1.01	1.11	1.00
		0.25	1.04	1.00	1.01	0.00	0.00
200	100	1	5.09	1.00	1.00	1.06	1.00
		0.25	1.05	0.66	0.73	0.04	0.00
200	200	1	5.52	1.03	1.03	1.11	1.00
		0.25	1.51	1.00	1.01	0.00	0.00
200	300	1	5.34	1.00	1.01	1.06	1.00
		0.25	2.19	1.00	1.00	0.00	0.00

Table 4. Average efficient detect rate under single change-point scenarios through SBM 1.

m	n	ρ	CP-TWAVG	CP-TWSBM	CP-TWMNBS	CP-GRA	CP-DMNBS
100	100	1	1.00	1.00	1.00	1.00	1.00
		0.25	0.97	0.94	0.95	0.00	0.00
100	200	1	1.00	1.00	1.00	1.00	1.00
		0.25	1.00	1.00	1.00	0.00	0.00
100	300	1	1.00	1.00	1.00	1.00	1.00
		0.25	1.00	1.00	1.00	0.00	0.00
200	100	1	1.00	1.00	1.00	1.00	1.00
		0.25	0.88	0.65	0.70	0.03	0.00
200	200	1	1.00	1.00	1.00	1.00	1.00
		0.25	1.00	1.00	1.00	0.00	0.00
200	300	1	1.00	1.00	1.00	1.00	1.00
		0.25	1.00	1.00	1.00	0.00	0.00

Table 5. Average Boysen distances $\varepsilon_1, \varepsilon_2$ under single change-point scenarios through SBM 1.

m	n	ρ		CP-TWAVG	CP-TWSBM	CP-TWMNBS	CP-GRA	CP-DMNBS
100	100	1	ε_1	35.16	0.39	0.39	1.53	0.03
			ε_2	0.00	0.00	0.00	0.00	0.03
		0.25	ε_1	1.62	0.39	0.92	-	-
			ε_2	0.13	0.12	0.12	-	-
100	200	1	ε_1	36.09	0.39	0.39	1.80	0.00
			ε_2	0.00	0.00	0.00	0.00	0.00
		0.25	ε_1	0.91	0.00	0.19	-	-
			ε_2	0.00	0.00	0.00	-	-
100	300	1	ε_1	35.83	0.31	0.31	2.18	0.00
			ε_2	0.00	0.00	0.00	0.00	0.00
		0.25	ε_1	0.93	0.00	0.36	-	-
			ε_2	0.00	0.00	0.00	-	-
200	100	1	ε_1	78.46	0.00	0.00	3.22	0.08
			ε_2	0.00	0.00	0.00	0.06	0.08
		0.25	ε_1	11.51	1.35	3.60	38.00	-
			ε_2	1.34	0.34	1.31	27.33	-
200	200	1	ε_1	80.86	1.60	1.60	3.88	0.00
			ε_2	0.00	0.00	0.00	0.00	0.00
		0.25	ε_1	23.31	0.01	0.41	-	-
			ε_2	0.01	0.01	0.01	-	-
200	300	1	ε_1	78.86	0.00	0.45	2.78	0.00
			ε_2	0.00	0.00	0.00	0.00	0.00
		0.25	ε_1	48.20	0.00	0.00	-	-
			ε_2	0.00	0.00	0.00	-	-

Note: the dash "-" means there is no change-points detected.

(1) Coummunity switching: $P'_{i,\cdot} = P_{j,\cdot}, P'_{\cdot,i} = P_{\cdot,j}, P'_{j,\cdot} = P_{i,\cdot}, P'_{\cdot,j} = P_{\cdot,i}$.

(2) Community merging: $P'_{i,\cdot} = P_{j,\cdot}, P'_{\cdot,i} = P_{\cdot,j}$.

(3) Community changing: Regenerate $P'_{i,j}$ from Graphon 4.

Then the dynamic networks $\{A_t\}_{t=1}^m$ for multiple change-points are designed as follows. $\mathcal{M}_1$ and $\mathcal{M}_2$ are two sets with $\lfloor n/3 \rfloor$ nodes randomly chosen from $\{1, 2, \ldots, n\}$. For $t = 1, 2, \ldots, m/4$, A_t is generated from P_1 by Graphon 2. For $t = m/4 + 1, \ldots, m/2$, A_t is generated from P_2 changed from P_1 by community switching. For $t = m/2 + 1, \ldots, 3m/4$, A_t is generated from P_3 changed from P_2 by community merging. For $t = 3m/4 + 1, \ldots, m$, A_t is generated from P_4 changed from P_3 by community changing. The results are illustrated in Tables 6–8.

The reports suggest that CP-TWMNBS performs the best in terms of the number, efficiency and accuracy of change-point estimation. CP-TWSBM enjoys reasonably good behavior when $m = 100$ while encounters some false positives when m increases to 200. As for CP-TWAVG, although the estimated change-points number $\hat{\mathcal{J}}$ in Table 6 are not far away from real value 3 and the efficient detect rates in Table 7 are all equal to 1, the Boysen distances in Table 8 are sometimes too large to be accepted, i.e., the location error can not be controlled stably.

On the other hand, CP-GRA detection suffers greatly under-estimating the change-points, especially when $\rho = 0.25$, there is no change-point detected in all cases. It happens similarly to CP-DMNBS detection when $\rho = 0.25$, so CP-DMNBS is also not the ideal for this scenario even though it is powerful when the networks are dense.

Overall, the numerical experiments clearly demonstrate the superior performance of CP-TWMNBS detection over other detect methods for all simulation scenarios with CP-TWSBM method coming in second. CP-TWMNBS detection provides robust and stable performance across all experiments with more accurate $\hat{\mathcal{J}}$, higher efficient detection and smaller Boysen distances.

5. Data analysis

In this section, we analyze the performance of the proposed TW_1-type method for two-sample test and TW_1-type change-point detection using two real datasets. The first dataset used for the two-sample test comes from the Centers of Biomedical Research Excellence (COBRE) and the second dataset used for change-point detection is from MIT Reality Mining (RM) (Eagle et al., 2009).

Table 6. Average estimated change-points number $\hat{J}$ under three change-points scenarios.

m	n	ρ	CP-TWAVG	CP-TWSBM	CP-TWMNBS	CP-GRA	CP-DMNBS
100	100	1	3.00	3.00	3.00	0.31	3.00
		0.25	1.92	3.40	2.99	0.00	0.02
100	200	1	3.00	3.00	3.00	2.10	3.00
		0.25	3.00	3.03	3.00	0.00	0.15
100	300	1	3.00	3.00	3.00	0.00	3.00
		0.25	3.00	3.00	3.00	0.00	1.52
200	100	1	3.16	3.00	3.00	2.29	3.02
		0.25	2.20	5.35	2.96	0.00	0.07
200	200	1	3.37	3.00	3.00	1.06	3.01
		0.25	3.00	4.57	3.01	0.00	1.62
200	300	1	3.57	3.01	3.00	0.11	3.00
		0.25	3.00	4.55	3.00	0.00	1.95

Table 7. Average efficient detect rate under three change-points scenarios.

m	n	ρ	CP-TWAVG	CP-TWSBM	CP-TWMNBS	CP-GRA	CP-DMNBS
100	100	1	1.00	1.00	1.00	0.13	1.00
		0.25	1.00	1.00	1.00	0.00	0.02
100	200	1	1.00	1.00	1.00	1.00	1.00
		0.25	1.00	1.00	1.00	0.00	0.15
100	300	1	1.00	1.00	1.00	0.00	1.00
		0.25	1.00	1.00	1.00	0.00	0.96
200	100	1	1.00	1.00	1.00	0.81	1.00
		0.25	1.00	1.00	1.00	0.00	0.07
200	200	1	1.00	1.00	1.00	0.39	1.00
		0.25	1.00	1.00	1.00	0.00	0.98
200	300	1	1.00	1.00	1.00	0.06	1.00
		0.25	1.00	1.00	1.00	0.00	1.00

Table 8. Average Boysen distances $\varepsilon_1, \varepsilon_2$ under three change-points scenarios.

m	n	ρ		CP-TWAVG	CP-TWSBM	CP-TWMNBS	CP-GRA	CP-DMNBS
100	100	1	ε_1	0.00	0.01	0.00	8.69	0.02
			ε_2	0.00	0.01	0.00	34.31	0.02
		0.25	ε_1	0.06	5.50	0.15	-	0.00
			ε_2	26.99	0.39	0.40	-	50.00
100	200	1	ε_1	0.00	0.00	0.00	1.17	0.00
			ε_2	0.00	0.00	0.00	25.10	0.00
		0.25	ε_1	0.00	0.45	0.00	-	0.07
			ε_2	0.00	0.00	0.00	-	50.07
100	300	1	ε_1	0.00	0.00	0.00	-	0.00
			ε_2	0.00	0.00	0.00	-	0.00
		0.25	ε_1	0.00	0.00	0.00	-	0.03
			ε_2	0.00	0.00	0.00	-	34.90
200	100	1	ε_1	4.70	0.00	0.00	14.72	0.69
			ε_2	0.00	0.00	0.00	53.96	0.16
		0.25	ε_1	0.08	29.51	0.67	-	0.43
			ε_2	40.01	0.51	3.30	-	79.00
200	200	1	ε_1	11.27	0.00	0.00	15.72	0.35
			ε_2	0.00	0.00	0.00	61.03	0.04
		0.25	ε_1	0.00	27.64	0.30	-	0.04
			ε_2	0.00	0.03	0.00	-	65.83
200	300	1	ε_1	17.05	0.33	0.00	11.17	0.00
			ε_2	0.00	0.00	0.00	89.33	0.00
		0.25	ε_1	0.00	27.85	0.00	-	0.07
			ε_2	0.00	0.02	0.00	-	52.47

Note: the dash "-" means there is no change-points detected.

5.1. *Two-sample test with real data example*

Raw anatomical and functional scans from 146 subjects of 72 patients with schizophrenia (SCZ) and 74 healthy controls (HCs) can be downloaded from a public database (`http://fcon_1000.projects.nitrc.org/indi/retro/cobre.html`). In this paper, we use the processed connectomics dataset in Relión et al. (2019). After a series of pre-processing steps, Relión et al. (2019) keeps 54 SCZ and 70 HC subjects for analysis and chooses 264 brain regions of interest as the nodes. For each of the 263 nodes with every other node, they applies Fisher's R-to-Z transformation to the cross-correlation matrix of Pearson r-values.

In our study, we perform the Z-to-R inverse transformation to their dataset to get the original cross-correlation matrix of Pearson r-values, which is denoted as R. To analyze graphical properties of these brain functional networks, we need to create an adjacency matrix A from R. We set A_{ij} to be 1 if R_{ij} exceeds a threshold T and A_{ij} to be 0 otherwise. There is no generally accepted way to identify an optimal threshold for this graph construction procedure, we decide to set T varied between 0.3 and 0.7 with step of 0.05.

For each threshold T, two situations are considered for the two-sample test. In the first situation, we randomly divide HC into 2 groups with sample sizes $m_1 = m_2 = 35$ and calculate the average null hypothesis reject rates of TW_1-MNBS test, TW_1-AVG test, TW_1-SBM test, χ^2-type test, and N-type test through 100 repeated simulations. In the second situation, we apply the same test methods above to two groups of SCZ and HC directly and compare their average null hypothesis reject rates. In both cases, the significance level is set to be 0.05. The results are shown in Tables 9 and 10 respectively.

Table 9. Average H_0 reject rate of test over HC group over 100 simulations.

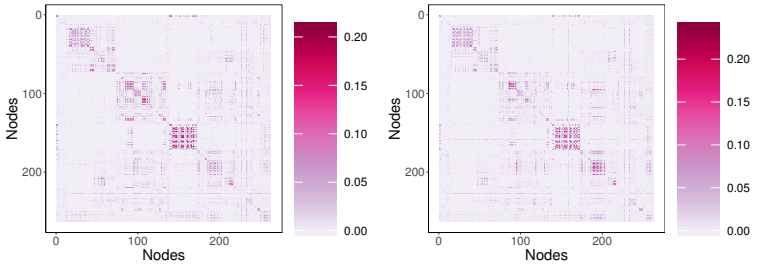
T	0.30	0.35	0.40	0.45	0.50	0.55	0.60	0.65	0.70
TW_1-AVG	1	1	1	1	0.80	0.67	0.57	0.50	0.44
TW_1-SBM	1	1	1	1	1	1	1	1	1
TW_1-MNBS	1	1	1	1	1	0	0	1	1
χ^2-type	1	1	0	0	0	0	0	0	0
N-type	1	1	1	0	0	0	0	0	0

Table 10. Average H_0 reject rate of test over SCZ and HC groups.

T	0.30	0.35	0.40	0.45	0.50	0.55	0.60	0.65	0.70
TW_1-AVG	1	1	1	1	1	0	0	0	0
TW_1-SBM	1	1	1	1	1	1	1	1	1
TW_1-MNBS	1	1	1	1	1	1	1	1	1
χ^2-type	0	0	0	0	0	0	0	0	0
N-type	1	1	1	1	1	1	1	1	1

To investigate the performance of the tests, we need to compare the type I error in Table 9 and

the power result in Table 10 together. Table 9 shows that TW_1-type tests based on SBM and AVG have poor performance for the test over HC group because the reject rates all exceed 0.05 and even equal to 1. From Table 10, it is found that χ^2-type test loses power for the test over SCZ and HC groups, where the reject rates are all 0. Only TW_1-type test based on MNBS when $T = 0.55, 0.60$ and N-type test when $T \geq 0.45$ can perform well in both situations. In addition, applying MNBS, we illustrate the adjacency matrices of subject-specific networks of HC and SCZ groups when $T = 0.60$ in Figure 3. One can find that the two groups do have differences in the network structure.



(a) HC (b) SCZ

Figure 3. Adjacency matrices estimated by MNBS for HC and SCZ groups.

5.2. *Change-point detection in dynamic networks*

In this section, we apply CP-TWMNBS, CP-TWAVG, CP-TWSBM, CP-GRA, and CP-DMNBS detections to perform change-point detection for a phone-call network data extracted from RM dataset. The data is collected through an experiment conducted by the MIT Media Laboratory following 106 MIT students and staff using mobile phones with preinstalled software that can record and send call logs from 2004 to 2005 academic year. Note that this is different from the MIT proximity network data considered in Zhao et al. (2019) which is based on the bluetooth scans instead of phone calls. In this analysis, we are interested in whether phone call patterns changed during this time, which may reflect a change in relationship among these subjects. 94 of the 106 RM subjects completed the survey, we remain records only within these participants and filter records before 07/20/2004 due to the extreme scarcity of sample before that time. Then there remains 81 subjects left and we construct dynamic networks among these subjects by day. For each day, construct a network with the subjects as nodes and a link between two subjects if they had at least one call on that day. We encode the network of each day by an adjacency matrix, with 1 for element (i, j) if there is an edge between subject i and subject j, and 0 otherwise. Thus, there are in total 310 days from 07/20/2004 to 06/14/2005. The calendar of events is included in the appendix. We claim that an estimated change-point is reasonable if it is at most three days away from the real

dates the event lasts.

We first choose $h = 7$ and Figure 4 plots the results of different methods on the dynamic networks. The purple shadow areas mark time intervals from the beginning to the end of events continue on MIT academic calendar 2004–2005, which can be used as references for the estimated change-points' occurrences. The red lines in Figure 4 are the estimated change-points applying different detect methods.

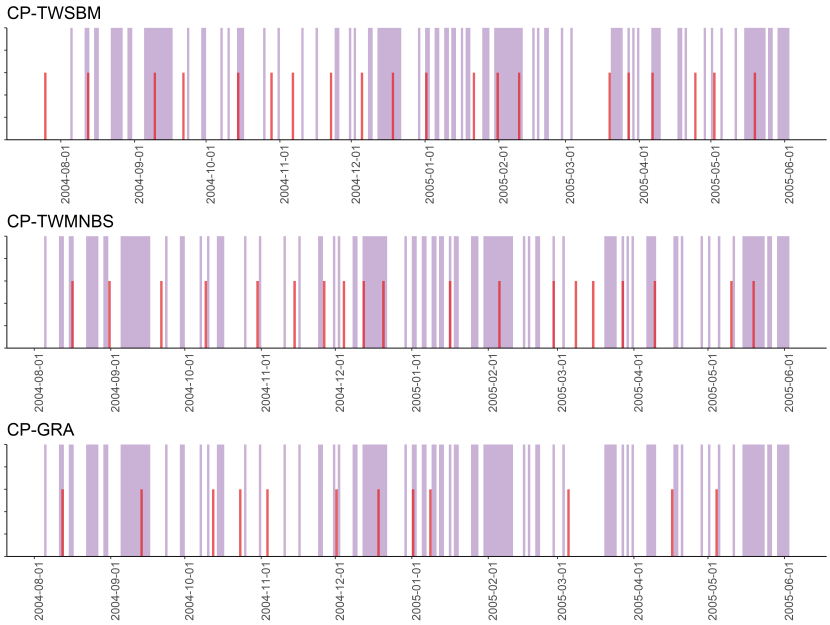


Figure 4. Calendar time intervals of events and estimated change-points.

It turns out that CP-TWAVG and CP-DMNBS detections either do not work well or detect no change-point. CP-TWSBM method detects 20 change-points, CP-TWMNBS method detects 19 change-points, while CP-GRA detection detects 12 change-points. When comparing the estimated change-points to intervals of calendar events, we see that they align each other the best by using CP-TWMNBS detection and then CP-TWSBM detection, whereas there are more estimated change-points by CP-GRA detection that can not be explained.

However, it's observed that some of the change-points detected by CP-TWSBM and CP-TWMNBS methods can be a little trivial. For example, CP-TWMNBS detected a change-point occurred at around 01/09/2004, which is near event "English Evaluate Test for International Students" in the calendar. To ignore the less significant events, we only consider the seemingly major events displayed in bold in the calendar as possible reasons for estimated change-points and set $h = 14$, which corresponds to 2 weeks. The details are reported in Table 11. The CP-TWMNBS and CP-TWSBM methods detect 9 change-points, CP-GRA method detects 13 change-points. Notably CP-GRA method still labels more trivial change-points away from the important events. Based on the results,

it is most likely valid in saying that CP-TWSBM and CP-TWMNBS detections are more reliable.

Table 11. Estimated change-points by different methods for MIT phone data.

CP-TWSBM	02/08/2004	08/09/2004	12/10/2004	15/11/2004	27/12/2004	03/02/2005	19/02/2005
	23/03/2005	03/05/2005					
CP-TWMNBS	10/08/2004	27/09/2004	17/10/2004	20/11/2004	05/12/2004	24/12/2004	13/02/2005
	10/04/2005	04/05/2005					
CP-GRA	13/08/2004	01/09/2004	14/09/2004	28/09/2004	13/10/2004	04/11/2004	18/11/2004
	02/12/2004	19/12/2004	09/01/2005	06/03/2005	17/04/2005	05/05/2005	

6. Conclusion

We consider the problem of hypothesis testing on whether two populations of networks defined on a common vertex set are from the same distribution. Two-sample testing on populations of networks is a challenging task especially when the the number of nodes is large. We propose a general TW_1-type test (which is later adapted to a change-point detection procedure in dynamic networks), derive its asymptotic distribution and asymptotic power. The test statistics utilizes some plugin estimates for the link probability matrices and properties of the resulting tests with various estimates are discussed by evaluating and comparing TW_1-type tests based on MNBS, AVG, SBM theoretically, and numerically with both simulated and real data. From the simulation study, we see that the proposed TW_1-type test based on MNBS performs the best and yields robust results even when the structure is sparse. In addition, we provide a significant modification of the two-sample network test for change-point detection in dynamic networks. Simulation and real data analyses show that the procedure is consistent, principled and practically viable.

Acknowledgements

The work of Li Chen was supported by the China Scholarship Council under Grant 201806240032 and the Fundamental Research Funds for the Central Universities, Southwest Minzu University under grant 2021NQNCZ02. The work of Jie Zhou was supported in part by the National Natural Science Foundation of China under grants 61374027 and 11871357, and in part by the Sichuan Science and Technology Program under grant 2019YJ0122. Lizhen Lin acknowledges the generous support from NSF grants IIS 1663870, DMS Career 1654579, DMS 2113642 and a DARPA grant N66001-17-1-4041.

The appendix mainly includes theorem proofs omitted and the academic calendar of MIT we use in the paper.

Appendix A. Preliminaries

Proposition A.1 (Hoeffding's inequality (Hoeffding, 1963)): *If $X_1, X_2, \ldots, X_m$ are independent random variables and $a_i \le X_i \le b_i (i = 1, 2, \ldots, m)$, then for $t > 0$,*

$$P\left(\bar{X} - \mu \ge t\right) \le \exp\left\{-\frac{2m^2t^2}{\sum_{i=1}^m (b_i - a_i)^2}\right\},$$

where $\bar{X} = \frac{1}{m}\sum_{i=1}^m X_i,\ \mu = E(\bar{X})$.

Proposition A.2 (Bernstein's inequality (Bernstein, 1946)): *Let $X_1, X_2, \ldots, X_m$ be independent zero-mean random variables. Suppose that $|X_i| \le M$ with probability 1 for all i. Then for all positive t, we have*

$$P\left(\sum_{i=1}^m X_i > t\right) \le \exp\left\{-\frac{\frac{1}{2}t^2}{\sum_{i=1}^m E(X_i^2) + \frac{1}{3}Mt}\right\}.$$

For a sequence of independent Bernoulli random variables where $X_i \sim \text{Bernoulli}(p)$, by Proposition A.1 we have

$$P\big(\,|\bar{X} - p| \ge t\big) \le 2\exp\big\{-2mt^2\big\}.$$

Similarly, by Proposition A.2, we have

$$P\big(\,|\bar{X} - p| > t\big) \le 2\exp\left\{-\frac{\frac{1}{2}mt^2}{p(1-p) + \frac{1}{3}t}\right\}.$$

Lemma A.3 (Asymptotic distributions of $\lambda_1(Z)$ and $\lambda_n(Z)$): *For Z defined in (4) in subsection 2.3, we have*

$$n^{2/3}[\lambda_1(Z) - 2] \rightsquigarrow TW_1,\ n^{2/3}[-\lambda_n(Z) - 2] \rightsquigarrow TW_1.$$

Proof. Let G be an $n \times n$ symetric matrix whose upper diagonal entries are independent normal with mean zero and variance $1/(n-1)$, and zero diagonal entries. Let $H_G = \sqrt{(n-1)/n}G$, according to Theorem 1.2 in Lee and Yin (2014), $n^{2/3}[\lambda_1(H_G) - 2]$ converges to TW_1 in distribution. For convenience and without ambiguity, we also use TW_1 to denote a random variable following the Tracy–Widom law with index 1. Then we have

$$\lambda_1(H_G) = 2 + n^{-2/3}TW_1 + o_p(n^{-2/3}).$$

Further,

$$\lambda_1(G) = \sqrt{\frac{n}{n-1}}\lambda_1(H_G) = \left[1 + O_n\left(n^{-1}\right)\right]\lambda_1(H_G) = 2 + n^{-2/3}TW_1 + o_p(n^{-2/3}),$$

which is equivalent to

$$n^{2/3}[\lambda_1(G) - 2] \rightsquigarrow TW_1.$$

Since the first and second moments of entries of Z and G are the same, it follows from Theorem 2.4 in Erdős et al. (2012) that $n^{2/3}[\lambda_1(Z) - 2]$ and $n^{2/3}[\lambda_1(G) - 2]$ have the same limiting distribution. Therefore,

$$n^{2/3}[\lambda_1(Z) - 2] \rightsquigarrow TW_1.$$

The same argument applies to $\lambda_n(Z)$.

□

Appendix B. Proof of Theorem 2.1

Under the null hypothesis H_0, we have $P_1 = P_2 \equiv P$, and it's not difficult to observe that

$$\hat{Z}_{ij} = \frac{\sqrt{\frac{1}{m_1}P_{ij}(1-P_{ij}) + \frac{1}{m_2}P_{ij}(1-P_{ij})}}{\sqrt{\frac{1}{m_1}\hat{P}_{1,ij}\left(1-\hat{P}_{1,ij}\right) + \frac{1}{m_2}\hat{P}_{2,ij}\left(1-\hat{P}_{2,ij}\right)}}Z_{ij}. \tag{B1}$$

Since

$$\sup_{i,j}|\hat{P}_{u,ij} - P_{ij}| = o_p(n^{-2/3}), \tag{B2}$$

for the numerator in (B1), utilizing the Taylor Expansion, we have

$$\begin{aligned}
&\sqrt{\frac{1}{m_1}P_{ij}(1-P_{ij}) + \frac{1}{m_2}P_{ij}(1-P_{ij})} \\
&= \sqrt{\frac{m_1+m_2}{m_1m_2}P_{ij}(1-P_{ij})} \\
&= \sqrt{\frac{m_1+m_2}{m_1m_2}}\left[\sqrt{\hat{P}_{1,ij}\left(1-\hat{P}_{1,ij}\right)} + O_n\left(P_{ij} - \hat{P}_{1,ij}\right)\right] \\
&= \sqrt{\frac{m_1+m_2}{m_1m_2}}\left[\sqrt{\hat{P}_{1,ij}\left(1-\hat{P}_{1,ij}\right)} + o_p(n^{-2/3})\right] \\
&= \sqrt{\frac{1}{m_1}\hat{P}_{1,ij}\left(1-\hat{P}_{1,ij}\right) + \frac{1}{m_2}\hat{P}_{1,ij}\left(1-\hat{P}_{1,ij}\right)} + \sqrt{\frac{m_1+m_2}{m_1m_2}}o_p(n^{-2/3}),
\end{aligned}$$

where the third equality is obtained by condition (B2).

Without loss of gernerality, assume $\hat{P}_{1,ij}\big(1-\hat{P}_{1,ij}\big) \le \hat{P}_{2,ij}\big(1-\hat{P}_{2,ij}\big)$, then

$$\begin{aligned} &\sqrt{\frac{1}{m_1}P_{ij}(1-P_{ij})+\frac{1}{m_2}P_{ij}(1-P_{ij})} \\ &\le \sqrt{\frac{1}{m_1}\hat{P}_{1,ij}\big(1-\hat{P}_{1,ij}\big)+\frac{1}{m_2}\hat{P}_{2,ij}\big(1-\hat{P}_{2,ij}\big)}+\sqrt{\frac{m_1+m_2}{m_1m_2}}o_p(n^{-2/3}). \end{aligned} \tag{B3}$$

Similarily, we have

$$\begin{aligned} &\sqrt{\frac{1}{m_1}\hat{P}_{1,ij}\big(1-\hat{P}_{1,ij}\big)+\frac{1}{m_2}\hat{P}_{2,ij}\big(1-\hat{P}_{2,ij}\big)} \\ &\le \sqrt{\frac{1}{m_1}P_{ij}(1-P_{ij})+\frac{1}{m_2}P_{ij}(1-P_{ij})}+\sqrt{\frac{m_1+m_2}{m_1m_2}}o_p(n^{-2/3}). \end{aligned} \tag{B4}$$

From (B3) and (B4),

$$\begin{aligned} &\sqrt{\frac{1}{m_1}P_{ij}(1-P_{ij})+\frac{1}{m_2}P_{ij}(1-P_{ij})} \\ &= \sqrt{\frac{1}{m_1}\hat{P}_{1,ij}\big(1-\hat{P}_{1,ij}\big)+\frac{1}{m_2}\hat{P}_{2,ij}\big(1-\hat{P}_{2,ij}\big)}+\sqrt{\frac{m_1+m_2}{m_1m_2}}o_p(n^{-2/3}). \end{aligned} \tag{B5}$$

Combining (B5) with (B1), we have

$$\hat{Z}-Z = M\circ Z, \tag{B6}$$

where M is an $n\times n$ matrix whose elements $M_{ij}=o_p(n^{-2/3})$ and the notation $\circ$ denotes the Hadamard (element-wise) product of two matrices.

One has

$$\begin{aligned} \|\hat{Z}-Z\|_{op} &= \|M\circ Z\|_{op} \\ &= \sup_{\substack{\|x\|_2=1,\\ x\in\mathbb{R}^n}} \|(M\circ Z)x\|_2 \\ &= \sup_{\substack{\|x\|_2=1,\\ x\in\mathbb{R}^n}} \sqrt{\sum_{i=1}^{n}\left(\sum_{j=1}^{n}M_{ij}Z_{ij}x_j\right)^2}, \\ &= \sqrt{\sum_{i=1}^{n}\left(\sum_{j=1}^{n}M_{ij}Z_{ij}x_j^*\right)^2}, \end{aligned} \tag{B7}$$

where $\|\cdot\|_{op}$ denotes the operator norm of a matrix, $\|\cdot\|_2$ is the Euclidean norm of a vector, and x^* is a unit eigenvector of the largest singular of $M\circ Z$.

Define an $n \times n$ symmetric matrix as M^* and a unit vector as x'. Consider the last equality of (B7), let

$$M_{ij}^* = \begin{cases} M_{ij}, & Z_{ij}x_j^* \geq 0, \\ -M_{ij}, & Z_{ij}x_j^* < 0, \end{cases}$$

and

$$x_j' = \begin{cases} x_j^*, & Z_{ij}x_j^* \geq 0, \\ -x_j^*, & Z_{ij}x_j^* < 0. \end{cases}$$

Therefore, we have

$$\begin{aligned} \|\hat{Z} - Z\|_{op} &= \sqrt{\sum_{i=1}^{n} \left(\sum_{j=1}^{n} M_{ij}^* Z_{ij} x_j' \right)^2} \\ &\leq (\sup_{i,j} |M_{ij}^*|) \sqrt{\sum_{i=1}^{n} \left(\sum_{j=1}^{n} Z_{ij} x_j' \right)^2} \\ &\leq (\sup_{i,j} |M_{ij}^*|) \|Z\|_{op}. \end{aligned} \tag{B8}$$

The first inequality in (B8) holds true since $Z_{ij}^* x_j'$ are non-negative for all i and j. In addition, Z is a Wigner matrix and from Corollary 2.3.6 in Tao (2012), the norm of Z satisties

$$\|Z\|_{op} = O_p(1).$$

The meaning of notation $O_p(\cdot)$ is as follows: For two sequences of real numbers $\{x_n\}$ and $\{y_n\}$, we write $y_n = O_p(x_n)$ if for any $\varepsilon > 0$, there exist finite $C > 0$ and $N > 0$ such that $P\big(\big|\frac{y_n}{x_n}\big| > C\big) < \varepsilon$ for any $n > N$.

It is noted that $M_{ij}^* = o_p(n^{-2/3})$, so

$$\|\hat{Z} - Z\|_{op} \leq o_p(n^{-2/3}).$$

Then

$$|\lambda_1(\hat{Z}) - \lambda_1(Z)| \leq o_p(n^{-2/3}). \tag{B9}$$

Combining (B9) with Lemma A.3, we have

$$n^{2/3}[\lambda_1(\hat{Z}) - 2] \rightsquigarrow TW_1.$$

Similarly, we can prove

$$n^{2/3}[-\lambda_n(\hat{Z}) - 2] \rightsquigarrow TW_1.$$

Appendix C. Proof of Corollary 2.3

$$\begin{aligned} P(T_{TW_1} \geq \tau_{\alpha/2}) &\leq P\big(n^{2/3}[\lambda_1(\hat{Z}) - 2] \geq \tau_{\alpha/2}\big) + P\big(n^{2/3}[-\lambda_n(\hat{Z}) - 2] \geq \tau_{\alpha/2}\big) \\ &= \alpha/2 + o_n(1) + \alpha/2 + o_n(1) \\ &= \alpha + o_n(1). \end{aligned}$$

Appendix D. Proof of of Corollary 2.4

Define a matrix $W \in \mathbb{R}^{n\times n}$ with zero diagonal and for any $i \neq j$,

$$W_{ij} = \frac{(P_{1,ij} - P_{2,ij}) - (\bar{A}_{1,ij} - \bar{A}_{2,ij})}{\sqrt{(n-1)\Big[\frac{1}{m_1}P_{1,ij}(1 - P_{1,ij}) + \frac{1}{m_2}P_{2,ij}(1 - P_{2,ij})\Big]}}.$$

Recall the definitions of $Z, \hat{Z}$ and $\tilde{Z}$ given by (4), (5) and (9) in subsection 2.3 respectively, from (B6), it is easy to get

$$\hat{Z}_{ij} = [1 + o_p(n^{-2/3})](\tilde{Z}_{ij} - W_{ij}).$$

Thus

$$[1 + o_p(n^{-2/3})]\tilde{Z}_{ij} = \hat{Z}_{ij} + [1 + o_p(n^{-2/3})]W_{ij}.$$

This implies

$$\hat{Z} = \tilde{Z} \circ (J + D) - W \circ (J + D),$$

where J is an $n \times n$ matrix with every element equal to 1, and D is an $n \times n$ matrix with elements $D_{ij} = o_p(n^{-2/3})$. Similarly with the proof of Theorem 2.1, we can get $\sigma_1(\tilde{Z} \circ (J + D)) = \sigma_1(\tilde{Z})$,

$\sigma_1(W \circ (J + D)) = \sigma_1(W)$ with probability 1 as $n \to \infty$.

Applying the triangle inequality of spectral norm, we have

$$\sigma_1(\hat{Z}) \geq \sigma_1(\tilde{Z}) - \sigma_1(W)$$

with probability 1 as n tends to infinity. Noting that W is a mean zero matrix whose singular value can be bounded by using the TW_1 asymptotic distribution. Hence, for any $\beta \in (0, 1)$,

$$\begin{aligned} & P\big(\sigma_1(W) \leq 2 + n^{-2/3}\tau_\beta\big) \\ &= 1 - P\big(\sigma_1(W) > 2 + n^{-2/3}\tau_\beta\big) \\ &\geq 1 - \big[P\big(\lambda_1(W) > 2 + n^{-2/3}\tau_\beta\big) + P\big(-\lambda_n(W) > 2 + n^{-2/3}\tau_\beta\big)\big] \\ &= 1 - 2\beta + o_n(1). \end{aligned} \tag{D1}$$

Set $\tau_\beta = n^{2/3}[\sigma_1(\tilde{Z}) - 4] - \tau_{\alpha/2}$, and plug this in (D1), then we have

$$\begin{aligned} 1 - 2\beta + o_n(1) &\leq P\left(\sigma_1(W) \leq 2 + n^{-2/3}\big\{n^{2/3}[\sigma_1(\tilde{Z}) - 4] - \tau_{\alpha/2}\big\}\right) \\ &= P\left(2 + n^{-2/3}\tau_{\alpha/2} \leq \sigma_1(\tilde{Z}) - \sigma_1(W)\right) \\ &\leq P\left(2 + n^{-2/3}\tau_{\alpha/2} \leq \sigma_1(\hat{Z})\right) \\ &= P\big(n^{2/3}[\sigma_1(\hat{Z}) - 2] \geq \tau_{\alpha/2}\big) \\ &= P(T_{TW_1} \geq \tau_{\alpha/2}). \end{aligned}$$

Observe that if $n^{-2/3}[\sigma_1(\tilde{Z}) - 4]^{-1} \leq o_n(1)$, for a fixed $\alpha \in (0, 1)$, we have $\tau_\beta^{-1} = o_n(1)$, that is $\beta = o_n(1)$. Therefore,

$$P(T_{TW_1} \geq \tau_{\alpha/2}) = 1 + o_n(1).$$

Appendix E. Proof of Theorem 3.1

For any t that is not a change-point, since $t \in \mathcal{J}$, we have

$$\begin{aligned}
P(T_{TW_1}(t,h) > \triangle_{T_{TW_1}}) &= 1 - P(T_{TW_1}(t,h) \leq \triangle_{T_{TW_1}}) \\
&= 1 - \prod_{t' \in (t-h, t+h)} P(T_{TW_1}(t',h) \leq \triangle_{T_{TW_1}}) \\
&= 1 - \prod_{t' \in (t-h, t+h)} \big[1 - P(T_{TW_1}(t',h) > \triangle_{T_{TW_1}})\big] \\
&\leq 1 - \prod_{t' \in (t-h, t+h)} \big[1 - P(T_{TW_1}(t',h) > \tau_\alpha)\big] \\
&\leq 1 - (1-2\alpha)^{2h} + o_n(1) \\
&= 1/n + o_n(1) \to 0.
\end{aligned}$$

For any t that is a true change-point, under the alternative hypothesis, $n^{2/3}[\delta(t,h) - 4] \geq 2\tau_\alpha$. We have

$$\begin{aligned}
P(T_{TW_1}(t,h) > \triangle_{T_{TW_1}}) &= P\Big(n^{2/3}\big[\sigma_1\big(\hat{Z}(t,h)\big) - 2\big] > n^{2/3}[\delta(t,h) - 4] - \tau_\alpha\Big) \\
&= P\big(\sigma_1\big(\hat{Z}(t,h)\big) > \delta(t,h) - 2 - n^{-2/3}\tau_\alpha\big).
\end{aligned} \tag{E1}$$

Assume $P_1(t,h)$ and $P_2(t,h)$ are the true link probability matrices of groups $\{A_i\}_{i=t-h+1}^{t}$ and $\{A_i\}_{i=t+1}^{t+h}$. For proof convenience later, we denote matrices $B_1(t,h)$, $B_2(t,h)$, $V_2(t,h)$ all with zero diagonals and for all $i \neq j$,

$$B_{1,ij}(t,h) = \frac{P_{1,ij}(t,h) - P_{2,ij}(t,h)}{\sqrt{(n-1)\Big\{\frac{1}{h}\hat{P}_{1,ij}(t,h)\Big[1 - \hat{P}_{1,ij}(t,h)\Big] + \frac{1}{h}\hat{P}_{2,ij}(t,h)\Big[1 - \hat{P}_{2,ij}(t,h)\Big]\Big\}}},$$

$$B_{2,ij}(t,h) = \frac{[P_{1,ij}(t,h) - P_{2,ij}(t,h)] - [\bar{A}_{1,ij}(t,h) - \bar{A}_{2,ij}(t,h)]}{\sqrt{(n-1)\Big\{\frac{1}{h}\hat{P}_{1,ij}(t,h)\Big[1 - \hat{P}_{1,ij}(t,h)\Big] + \frac{1}{h}\hat{P}_{2,ij}(t,h)\Big[1 - \hat{P}_{2,ij}(t,h)\Big]\Big\}}},$$

$$V_{2,ij}(t,h) = \frac{[P_{1,i,j}(t,h) - P_{2,ij}(t,h)] - [\bar{A}_{1,ij}(t,h) - \bar{A}_{2,ij}(t,h)]}{\sqrt{(n-1)\Big\{\frac{1}{h}P_{1,ij}(t,h)\big[1 - P_{1,ij}(t,h)\big] + \frac{1}{h}P_{2,ij}(t,h)\big[1 - P_{2,ij}(t,h)\big]\Big\}}}.$$

Then the lower bound of $\sigma_1(t,h)$ can be obtained:

$$\begin{aligned}\sigma_1\big(\hat{Z}(t,h)\big) &\geq \sigma_1(B_1(t,h)) - \sigma_1(B_2(t,h)) \\ &= \big[\sigma_1(V_1(t,h)) - \sigma_1(V_2(t,h))\big]\,[1 + o_p(n^{-2/3})] \\ &\geq \delta(t,h) - 2 - n^{-2/3}\tau_\alpha,\end{aligned}$$

with probability at most $1 - 2\alpha + o_n(1)$. The last inequality follows by noting that $V_2(t,h)$ is a generalized Wigner matrix. Similarly with proof of Lemma A.3, we have $P\big(n^{2/3}\big[\sigma_1(V_2(t,h)) - 2\big] \leq \tau_\alpha\big) \geq 1 - 2\alpha + o_n(1)$. Combining this with (E1), we have

$$P(T_{TW_1}(t,h) > \triangle_{T_{TW_1}}) = 1 - 2\alpha + o_n(1) = (1 - 1/n)^{1/(2h)} + o_n(1) \to 1.$$

The above result implies that with probability of 1, all and only the change-points will be selected at the thresholding steps. Therefore, we have

$$\lim_{n\to\infty} P\big(\mathcal{J} = \hat{\mathcal{J}}\big) = 1.$$

Appendix F. Academic calendar of MIT 2004–2005

The academic calendar of MIT we use in this paper is illustrated as follows.

Table F1. Academic calendar of MIT from July 20, 2004 to June 14, 2005.

Date	Event
August 6, 2004	**Deadline for doctoral students to submit application for Fall Term Non-Resident status; Thesis due for September degree candidates**.
August 12, 2004	**Continuing students final deadline to pre-reg on-line**.
August 13, 2004	**Last day to go off the September degree list**.
August 16–17, 2004	Summer Session Final Exam Period.
August 23, 2004	**Grades due**.
August 27, 2004	Term Summaries of Summer Session Grades.
August 30, 2004	Graduate Student Orientation activities begin.
August 31, 2004	English Evaluation Test for International students.
September 6, 2004	Labor Day–Holiday.
September 7, 2004	**Registration day**.
September 8, 2004	**First day of classes**.
September 9–17, 2004	Physical Education Petition Period.
September 10, 2004	**Degree application deadline**.
September 14, 2004	Committee on Graduate School Policy Meeting.
September 15, 2004	Faculty officers recommend degrees to Corporation.
September 24, 2004	**Minor completion date**.
September 30, 2004	Last day to sing up family health insurance or waive individual coverage.
October 1, 2004	Deadline for completing Harvard cross-registration.
October 8, 2004	**Last day to add subjects to Registration**.
October 11, 2004	Columbus Day–Holiday.
October 15–17, 2004	Family Weekend.
October 2, 20046	Second quarter Physical Education classes begin.
November 1, 2004	Half-term subjects offered in second half of term begin.
November 11, 2004	Veteran's Day–Holiday.
November 17, 2004	**Last day to cancel subjects from Registration**.
November 25–26, 2004	Thanksgiving Vacation–Holiday.
December 1, 2004	**On-line pre-registration for Spring Term begins**.
December 3, 2004	**Subjects with no final/final exam**.
December 9, 2004	**Last day of classes**.

Date	Event
December 10, 2004	Last day to submit or change Advanced Degree Thesis Title.
December 13–17, 2004	**Final exam period**.
December 14–22, 2004	**Grade deadline**.
December 18, 2004	Winter Vacation begins–Holiday.
December 30, 2004	**Spring pre-registration deadline**.
January 2, 2005	Winter Vacation ends.
January 3, 2005	**Deadline for doctoral students to submit applications for Spring Term Non-Resident status**.
January 6, 2005	Term Summaries of Fall Term Grades.
January 7, 2005	**Thesis due**.
January 10, 2005	Second-Year and Third-Year Grades Meeting.
January 11, 2005	Fourth-Year Grades meeting; Committee on Graduate School Policy Meeting.
January 13, 2005	**Final deadline for continuing students to pre-reg on-line**.
January 14, 2005	**Thesis due**.
January 17, 2005	Martin Luther King, Jr. Day–Holiday.
January 19–20, 2005	C.A.P. deferred action meeting.
January 26, 2005	English Evaluation Test for International students.
January 26–28, 2005	Some advanced standing exams and postponed finals.
January 28, 2005	Last day of January Independent Activities Period.
January 31, 2005	**Registration day**.
February 1, 2005	**First day of classes**.
February 2–11, 2005	Physical Education Petition Period.
February 3, 2005	**Grades due**.
February 4, 2005	**Registration deadline**.
February 7, 2005	Term summaries of Grades for IAP.
February 8, 2005	Committee on Graduate School Policy Meeting.
February 11, 2005	C.A.P. February Degree Candidates Meeting.
February 16, 2005	Faculty Officers recommend degrees to Corporation.
February 18, 2005	**Minor completion date**.
February 21, 2005	Presidents Day–Holiday.
February 22, 2005	**Monday schedule of classes to be held**.
February 28, 2005	Last day to sing up for family health insurance or waive individual coverage.
March 4, 2005	**Last day to add subjects to Registration**.
March 21–25, 2005	Spring Vacation–Holiday.
March 28, 2005	Half-term subjects offered in second half of term begin.
March 30, 2005	Fourth quarter Physical Education classes begin.
April 1, 2005	Last day to submit or change Advanced Degree Thesis Title.
April 7–10, 2005	Campus Preview Weekend.
April 18–19, 2005	Patriots Day–Holiday.
April 21, 2005	**Last day to cancel subjects from Registration**.
April 29, 2005	**Thesis due**.
May 2, 2005	**On-line pre-registration for Fall Term and Summer Session begins**.
May 6, 2005	**Subjects with no final/final exam**.
May 12, 2005	**Last day of classes**.
May 16–20, 2005	**Final exam week**.
May 17–24, 2005	**Grade deadline**.
May 20, 2005	**Last day to go off the June degree list**.
May 26, 2005	**Department grades meetings**.
May 27, 2005	Fourth-Year Grades Meeting.
May 30, 2005	Memorial Day–Holiday.
May 31, 2005	**Fall pre-registration deadline**.
June 1, 2005	First-Year Grades Meeting.
June 2, 2005	Doctoral Hooding Ceremony.
June 3, 2005	**Commencement**.
June 14, 2005	C.A.P. deferred action meeting.

References

Amini, A. A. and Levina, E. (2018). On semidefinite relaxations for the block model. *The Annals of Statistics*, 46(1):149–179.

Ball, B., Karrer, B., and Newman, M. E. J. (2011). Efficient and principled method for detecting communities in networks. *Physical Review E*, 84(3). Art. ID 036103.

Bassett, D. S., Bullmore, E., Verchinski, B. A., Mattay, V. S., Weinberger, D. R., and Meyer-Lindenberg, A. (2008). Hierarchical organization of human cortical networks in health and schizophrenia. *The Journal of Neuroscience*, 28(37):9239–9248.

Bernstein, S. (1946). *The Theory of Probabilities*. Gastehizdat Publishing House, Moscow, Soviet Union.

Bhattacharya, R. and Lin, L. (2017). Omnibus CLTs for Fréchet means and nonparametric inference on non-euclidean spaces. *The Proceedings of the American Mathematical Society*, 145:413–428.

Bickel, P. J. and Chen, A. (2009). A nonparametric view of network models and Newman–Girvan and other modularities. *Proceedings of the National Academy of Sciences of the United States of America*, 106(50):21068–21073.

Bounova, G. and de Weck, O. (2012). Overview of metrics and their correlation patterns for multiple-metric topology analysis on heterogeneous graph ensembles. *Physical Review E*, 85. Art. ID 016117.

Boysen, L., Kempe, A., Liebscher, V., Munk, A., and Wittich, O. (2009). Consistencies and rates of convergence of jump-penalized least squares estimators. *The Annals of Statistics*, 37(1):157–183.

Cai, T., Li, H., Ma, J., and Xia, Y. (2019). Differential Markov random field analysis with an application to detecting differential microbial community networks. *Biometrika*, 106(2):401–416.

Chen, A., Cao, J., and Bu, T. (2010). Network tomography: Identifiability and Fourier domain estimation. *IEEE Transactions on Signal Processing*, 58(12):6029–6039.

Chen, H. and Zhang, N. (2015). Graph-based change-point detection. *The Annals of Statistics*, 43(1):139–176.

Chen, J. and Yuan, B. (2006). Detecting functional modules in the yeast protein–protein interaction network. *Bioinformatics*, 22(18):2283–2290.

Cline, M. S., Smoot, M., Cerami, E., Kuchinsky, A., Landys, N., Workman, C., Christmas, R., Avila-Campilo, I., Creech, M., Gross, B., Hanspers, K., Isserlin, R., Kelley, R., Killcoyne, S., Lotia, S., Maere, S., Morris, J., Ono, K., Pavlovic, V., Pico, A. R., Vailaya, A., Wang, P.-L., Adler, A., Conklin, B. R., Hood, L., Kuiper, M., Sander, C., Schmulevich, I., Schwikowski, B., Warner, G. J., Ideker, T., and Bader, G. D. (2007). Integration of biological networks and gene expression data using Cytoscape. *Nature Protocols*, 2(10):2366–2382.

Decelle, A., Krzakala, F., Moore, C., and Zdeborová, L. (2011). Asymptotic analysis of the stochastic block model for modular networks and its algorithmic applications. *Physical Review E*, 84(6). Art. ID 066106.

Durante, D., Dunson, D. B., and Vogelstein, J. T. (2017). Nonparametric Bayes modeling of populations of networks. *Journal of the American Statistical Association*, 112(520):1516–1530.

Eagle, N., Pentland, A. S., and Lazer, D. (2009). Inferring friendship network structure by using mobile phone data. *Proceedings of the National Academy of Sciences of the United States of America*, 106(36):15274–15278.

Erdős, L., Yau, H.-T., and Yin, J. (2012). Rigidity of eigenvalues of generalized Wigner matrices. *Advances in Mathematics*, 229(3):1435–1515.

Erdős, P. and Rényi, A. (1959). On random graphs. I. *Publicationes Mathematicae*, 6:290–297.

Fréchet, M. (1948). Les éléments aléatoires de nature quelconque dans un espace distancié. *Annales de L'Institut Henri Poincaré*, 10(4):215–310.

Ghoshdastidar, D., Gutzeit, M., Carpentier, A., and Von Luxburg, U. (2020). Two-sample hypothesis testing for inhomogeneous random graphs. *The Annals of Statistics*, 48(4):2208–2229.

Ghoshdastidar, D. and von Luxburg, U. (2018). Practical methods for graph two-sample testing. In *Advances in Neural Information Processing Systems*, pages 3019–3028, Montréal, Canada.

Ginestet, C. E., Li, J., Balanchandran, P., Rosenberg, S., and Kolaczyk, E. D. (2017). Hypothesis testing for network data in functional neuroimaging. *The Annals of Applied Statistics*, 11(2):725–750.

Hoeffding, W. (1963). Probability inequalities for sums of bounded random variables. *Journal of the American Statistical Association*, 58(301):13–30.

Hoff, P. D., Raftery, A. E., and Handcock, M. S. (2002). Latent space approaches to social network analysis. *Journal of the American Statistical Association*, 97(460):1090–1098.

Holland, P. W., Laskey, K. B., and Leinhardt, S. (1983). Stochastic blockmodels: First steps. *Social Networks*, 5(2):109–137.

Karrer, B. and Newman, M. E. J. (2011). Stochastic blockmodels and community structure in networks. *Physical Review E*, 83. Art. ID 016107.

Kolaczyk, E., Lin, L., Rosenberg, S., Walters, J., and Xu, J. (2020). Averages of unlabeled networks: Geometric characterization and asymptotic behavior. *Thes Annals of Statistics*, 48(1):514–538.

Kossinets, G. and Watts, D. J. (2006). Empirical analysis of an evolving social network. *Science*, 311(5757):88–90.

Kulig, A., Drożdż, S., Kwapień, J., and Oświęcimka, P. (2015). Modeling the average shortest-path length in growth of word-adjacency networks. *Physical Review E*, 91(3). Art. ID 032810.

Lee, J. O. and Yin, J. (2014). A necessary and sufficient condition for edge universality of wigner matrices. *Duke Mathematical Journal*, 163(1):117–173.

Lei, J. (2016). A goodness-of-fit test for stochastic block models. *The Annals of Statistics*, 44(1):401–424.

Leonardi, N. and Van De Ville, D. (2013). Tight wavelet frames on multislice graphs. *IEEE Transactions on Signal Processing*, 61(13):3357–3367.

Lovász, L. (2012). *Large Networks and Graph Limits*. American Mathematical Society, Providence, RI, USA.

Mukherjee, S. S., Sarkar, P., and Lin, L. (2017). On clustering network-valued data. In *Advances in Neural Information Processing Systems*, pages 7071–7081, Long Beach, CA, USA.

Niu, Y. S. and Zhang, H. (2012). The screening and ranking algorithm to detect dna copy number variations. *The Annals of Applied Statistics*, 6(3):1306–1326.

Relión, J. D. A., Kessler, D., Levina, E., and Taylor, S. F. (2019). Network classification with applications to brain connectomics. *The Annals of Applied Statistics*, 13(3):1648–1677.

Rohe, K., Chatterjee, S., and Yu, B. (2011). Spectral clustering and the high-dimensional stochastic block model. *The Annals of Statistics*, 39(4):1878–1915.

Snijders, T. A. B. and Baerveldt, C. (2003). A multilevel network study of the effects of delinquent behavior on friendship evolution. *Journal of Mathematical Sociology*, 27(2-3):123–151.

Tang, M., Athreya, A., Sussman, D. L., Lyzinski, V., Park, Y., and Priebe, C. E. (2017). A semi-parametric two-sample hypothesis testing problem for random graphs. *Journal of Computational and Graphical Statistics*, 26(2):344–354.

Tao, T. (2012). *Topics in Random Matrix Theory*. American Mathematical Society, Providence, RI, USA.

Tracy, C. A. and Widom, H. (1996). On orthogonal and symplectic matrix ensembles. *Communications in Mathematical Physics*, 177(3):727–754.

von Luxburg, U. (2007). A tutorial on spectral clustering. *Statistics and Computing*, 17(4):395–416.

Wolfe, P. J. and Olhede, S. C. (2013). Nonparametric graphon estimation. *arXiv:1309.5936*.

Zhang, B., Li, H., Riggins, R. B., Zhan, M., Xuan, J., Zhang, Z., Hoffman, E. P., Clarke, R., and Wang, Y. (2009). Differential dependency network analysis to identify condition-specific topological changes in biological networks. *Bioinformatics*, 25(4):526–532.

Zhang, Y., Levina, E., and Zhu, J. (2017). Estimating network edge probabilities by neighbourhood smoothing. *Biometrika*, 104(4):771–783.

Zhao, Z., Chen, L., and Lin, L. (2019). Change-point detection in dynamic networks via graphon estimation. *arXiv:1908.01823*.

Zou, C., Yin, G., Feng, L., and Wang, Z. (2014). Nonparametric maximum likelihood approach to multiple change-point problems. *The Annals of Statistics*, 42(3):970–1002.